

Ultrastrong coupling of high-frequency two-dimensional cyclotron plasma mode with a cavity photon

V. M. Muravev, P. A. Gusikhin, I. V. Andreev, and I. V. Kukushkin

Institute of Solid State Physics, RAS, Chernogolovka 142432, Russia

(Received 29 August 2012; revised manuscript received 1 December 2012; published 11 January 2013)

The microwave transmission of a two-dimensional electron stripe placed on a metallic patch resonator is studied. An ultrastrong coupling of the cyclotron plasmon with a resonator photon mode is identified in the regime, where the plasmon frequency is much greater than the photon frequency. In the zero magnetic field, it is established that the polariton frequency is determined exclusively by the resonator photon frequency and the electron system—resonator overlap factor. Polariton magnetodispersion is studied as a function of electron density, resonator sizes, and stripe dimensions.

DOI: [10.1103/PhysRevB.87.045307](https://doi.org/10.1103/PhysRevB.87.045307)

PACS number(s): 78.70.Gq, 73.20.Mf, 73.50.Mx, 78.67.De

I. INTRODUCTION

Light-matter interaction in solid-state systems has received considerable interest. Of particular interest is the strong coupling regime, where light and matter excitation lifetimes are so long that energy exchange can occur between them many times before the system decays back into its ground state. In solid-state devices, this regime has been realized for excitons in a semiconductor cavity,¹ intersubband transitions in quantum wells,² and quantum electrodynamics circuits based on Josephson junctions.³ Under such conditions, excitation dispersion curves exhibit an anticrossing behavior with a mode separation often referred to as Rabi splitting ($2\Omega_R$), analogous to the well-known vacuum Rabi splitting of atomic systems.⁴ Recently, special attention has been drawn to the case where Ω_R is of the same order of magnitude as the uncoupled excitation frequency; this regime has been termed the “ultrastrong coupling regime”.⁵ Numerous physical phenomena have been predicted in this ultrastrong coupling regime, including the parametric generation of nonclassical light and the new nonadiabatic cavity QED phenomena reminiscent of the dynamical Casimir effect.^{5–7}

Recently, the ultrastrong coupling of a coplanar microresonator photon mode with a two-dimensional electron system (2DES) cyclotron plasma mode has been observed with a record ratio $2\Omega_R/\omega_0 = 0.93$.^{8,9} Here, ω_0 is the frequency of the unperturbed resonator photon mode. Such a large cyclotron plasmon-photon coupling was caused by a high number of available excitations per unit volume in the 2DES and an almost unitary overlap factor α between the polarization medium and the coplanar photon mode. Research on cyclotron plasmon polaritons in the 2DES has an unmatched advantage: The frequency of material excitation $\sqrt{\omega_c^2 + \omega_p^2}$ (ω_c and ω_p are cyclotron and plasma frequencies, respectively) can be tuned over a wide range by simply sweeping the magnetic field or changing the electron density of the system.^{10–12} All these facts suggest that plasmon polaritons in 2DES are the system of choice in order to explore the ultrastrong coupling regime. In the present work, we experimentally address the cyclotron plasmon polariton spectrum in the previously unexplored regime $\omega_p \gg \omega_0$. The polariton magnetodispersion exhibits a strong dependence on the overlap factor α and the 2DES properties. Different overlap factors are realized by changing the size of the metallic patch resonator. We

note that the obtained data are of great importance for the practical realization of 2DES plasma polariton devices.^{13,14} This is owing to the fact that the present system possesses high tunability in the ultrastrong coupling regime.

II. EXPERIMENTAL TECHNIQUE

Experiments were performed on two types of commercially available $\text{Al}_{0.33}\text{Ga}_{0.67}\text{As}/\text{GaAs}$ heterostructures with a 20-nm-wide single quantum well located 200 nm below the crystal surface. Electron densities n_s for the structures were $4.7 \times 10^{11} \text{ cm}^{-2}$ and $2.75 \times 10^{11} \text{ cm}^{-2}$, with a transport mobility $\mu \approx 10^6 \text{ cm}^2/\text{V} \cdot \text{s}$ ($T = 4.2 \text{ K}$). Stripe-shaped mesas with lengths (L) of 1.4, 1, and 0.6 mm and widths (W) of 50, 100, and 150 μm were fabricated from this heterostructure. The stripe terminates in an Ohmic contact at both ends. Two 20- μm -wide metallic gate fingers are deposited on top of the mesa across the stripe [see Fig. 1(c) for a schematic illustration]. These gates excite and detect the polariton wave. The semiconductor chip has a form of $3 \times 1.5 \times 0.6 \text{ mm}^3$ parallelepiped. It is placed on a $a \times b$ metallic patch resonator, where a and b are the resonator sizes along and across the stripe, respectively. The resonator is fabricated on top of either a ceramic (with dielectric permittivity 10) or a teflon (with permittivity 2.5) substrate. Resonators of different dimensions, including $4 \times 4 \text{ mm}^2$, $8 \times 4 \text{ mm}^2$, and $10.8 \times 4 \text{ mm}^2$, were investigated to tune the coupling between the resonator and the 2DES. Microwave radiation with frequencies from 0.1 to 40 GHz was guided with a coaxial cable and transferred to the 2DES via a 50 Ω coplanar waveguide transmission line. The central conductor of this waveguide is bonded from one side to the central gate finger e [Fig. 1(c)], which serves as a polariton exciter. The central conductor is bonded to the end gate finger t from the other side, which collects the microwave signal transmitted through the 2DES stripe, and directs it onto a Schottky diode located outside the cryostat. The ground planes of the coplanar waveguide are connected to the adjacent Ohmic contacts S and D of the 2DES stripe. The microwave power at the entrance to the coax cable was about 1–10 μW . The sample is placed in a helium cryostat at the center of a superconducting solenoid. Experiments are carried out by applying a small magnetic field (0–1.5 T) perpendicular to the sample surface at $T = 4.2 \text{ K}$.

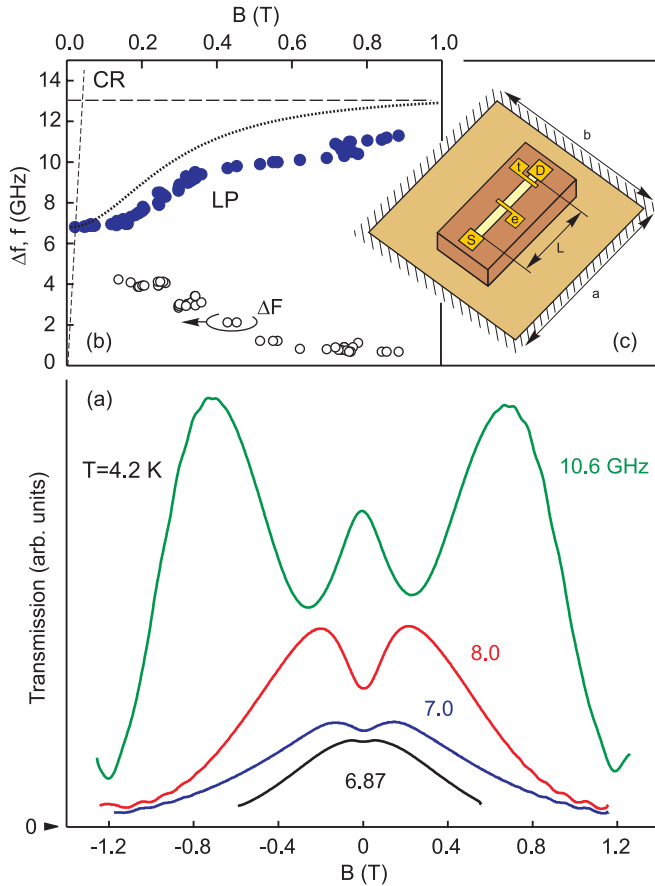


FIG. 1. (Color online) (a) Magnetic-field dependence of 2DES stripe transmission measured for several microwave frequency values ($n_s = 4.7 \times 10^{11} \text{ cm}^{-2}$, resonator $4 \times 4 \text{ mm}^2$ on a ceramic substrate). The zero on the vertical axis indicates the signal level in the absence of input microwave power. (b) Magnetic field values (filled dots) where transmission resonance occurs for a large set of microwave frequencies. The corresponding linewidths are plotted by open symbols as well. The dashed lines represent the cyclotron frequency (CR) and the resonator photon frequency. The dotted line shows the theoretical estimate of the polariton mode. (c) Schematic geometry of the semiconductor chip with a 2DES placed on top of the metallic patch resonator.

III. EXPERIMENTAL RESULTS

Figure 1(a) shows the magnetic-field dependence of the transmission of the 2DES stripe ($L = 1.4 \text{ mm}$, $W = 50 \mu\text{m}$) for several values of microwave frequency. The semiconductor chip was placed on top of the square $4 \times 4 \text{ mm}^2$ resonator on a ceramic substrate [Fig. 1(c)]. The zero on the vertical axis indicates the signal level in the absence of the input microwave power. Each curve shows a resonance that is symmetrical with respect to the zero magnetic field. This resonant peak corresponds to the excitation of hybrid photon-cyclotron plasmon mode with wave vector $q = \pi/a$, where $a = 4 \text{ mm}$ corresponds to the size of the side of the resonator. The resonance at zero magnetic field is a frequency insensitive background. We think that this background comes from the fact that the 2DES stripe plays the role of a nonresonant transmission line between excitation e and detection t gates. In order to gain further insight into the nature of the observed

mode, transmission experiments were repeated for a number of frequencies. Figure 1(b) shows the plot of the magnetic fields corresponding to the transmission maxima versus the microwave frequency (solid points). Only one branch of the polariton magnetodispersion is observed. The low-frequency branch originates at $B = 0 \text{ T}$ from a certain frequency ω_{LP} and tends to a photonic horizontal asymptotic value $\omega_0 = c/\sqrt{\varepsilon} \cdot \pi/a$ in the limit of large magnetic fields. Here, ε is the effective dielectric permittivity of the medium that surrounds the resonator. The precise value of ε was obtained from a theoretical simulation of electrodynamic response of the patch resonator with a semiconductor crystal on top of it. For the resonator under study, the effective permittivity is $\varepsilon = 8.4$. For comparison, we show on the same plot the magnetic-field dependence of the low-frequency polariton mode linewidth (open symbols). The polariton linewidth is obtained from the half width of the polariton resonance in B sweeps multiplied by the magnetodispersion slope. To calculate the half width of the resonance, we subtract nonresonant background from the transmission curve, and take the B -field difference between the polariton resonance maximum and half maximum on the resonance high magnetic field side. In the limit of large magnetic fields, the polariton linewidth is $\Delta f = 0.56 \text{ GHz}$, which corresponds to the resonator photon lifetime ($Q \approx 25$). At the resonant point $\omega_0 = \omega_c$, we may conclude that the polariton splitting $2\Omega_R/\omega_0$ derived only from the frequency position of the low-frequency polariton mode is not less than 0.5, indicating an ultrastrong coupling between the cyclotron plasmon and photon modes (Fig. 1).

We attempt to understand the polariton magnetodispersion behavior using a common approach based on the microscopic quantum theory of two independent coupled oscillators: the bare resonator photon mode and a bosonic cyclotron plasma excitation.¹⁵ This approach allows us to introduce an effective dielectric constant $\bar{\varepsilon}\omega^2/c^2 = q^2 = \varepsilon\omega_0^2/c^2$, where $\bar{\varepsilon}$ is described by the relation

$$\frac{1}{\bar{\varepsilon}} = \frac{\alpha}{\varepsilon_{2DES}(\omega)} + \frac{1-\alpha}{\varepsilon}. \quad (1)$$

Here, $\varepsilon_{2DES}(\omega) = \varepsilon[1 - \omega_p^2/(\omega^2 - \omega_c^2)]$ is the usual dissipationless Drude dielectric constant of the 2DES, $\omega_c = eB/m^*$ is the cyclotron frequency, m^* denoting the effective mass of 2D electrons, and α is the overlap factor between the polarization medium and the resonator photon mode. In the limit of $\alpha = 1$, the used theoretical approach recovers the homogeneous Hopfield model.¹⁶ For the system under study, ω_p represents the two-dimensional plasmon frequency with dispersion:¹⁷

$$\omega_p^2(k) = \frac{n_s e^2}{m^* \varepsilon_0 \varepsilon(k)} k, \quad (2)$$

where $k = \pi/W \times N$ ($N = 1, 3, 5 \dots$) is the wave vector of the plasmon and n_s is the density of the two-dimensional electrons. The permittivity of vacuum and the effective permittivity of the medium surrounding the 2DES stripe are denoted by ε_0 and $\varepsilon(k)$, respectively. For the 2DES stripe under study ($W = 50 \mu\text{m}$), the fundamental plasmon frequency is $\omega_p/2\pi = 117 \text{ GHz}$. This plasmon frequency is far larger than the unperturbed photon frequency $\omega_0/2\pi = 13 \text{ GHz}$ [Fig. 1(b)]. The theoretically predicted results based on Eq. (1)

with $\omega_p/2\pi = 117$ GHz, $\varepsilon = 8.4$, and $\alpha = 0.73$ are represented by the dashed line in Fig. 1(b). There exists a qualitative agreement between the theoretical and experimental results.

In the limit $\omega_p \ll \omega_0$, we note that the low-frequency polariton branch at the zero magnetic field starts from $\omega_{LP} = \omega_p$, while the upper frequency branch originates from $\omega_{UP} = \omega_0$. This particular case was realized in all previous experimental studies of cyclotron plasmon and intersubband plasmon polaritons.^{2,6,8,9,15} In the present experiments, we address the opposite limit $\omega_p \gg \omega_0$, which is particularly important for the construction of 2DES plasma polariton devices.^{13,14} In this limit, $\omega_{LP} = \omega_0\sqrt{1-\alpha}$ and $\omega_{UP} = \omega_p$ [Eq. (1)]. The polariton frequency ω_{LP} is determined exclusively by the photon frequency ω_0 and the overlap factor α . Physically, this situation corresponds to the creation of a complex excitation in the system, i.e., a photon dressed by the cloud of electrons. In the remainder of the manuscript, we will corroborate this picture of a low-frequency polariton branch by measuring its dependence on the 2DES stripe and resonator parameters.

Figure 2 shows a plot of the magnetic fields for transmission maxima versus microwave frequency for three types of resonators placed on a teflon substrate: 4×4 mm², 8×4 mm² ($a = 8$ mm, $b = 4$ mm), and 10.8×4 mm². The stripe dimensions ($L = 1.4$ mm, $W = 50$ μ m) and the density of the 2DES (4.7×10^{11} cm⁻²) have been maintained constant for all three cases. The stripe was oriented along the resonator. The change in the longitudinal resonator size a drastically affects

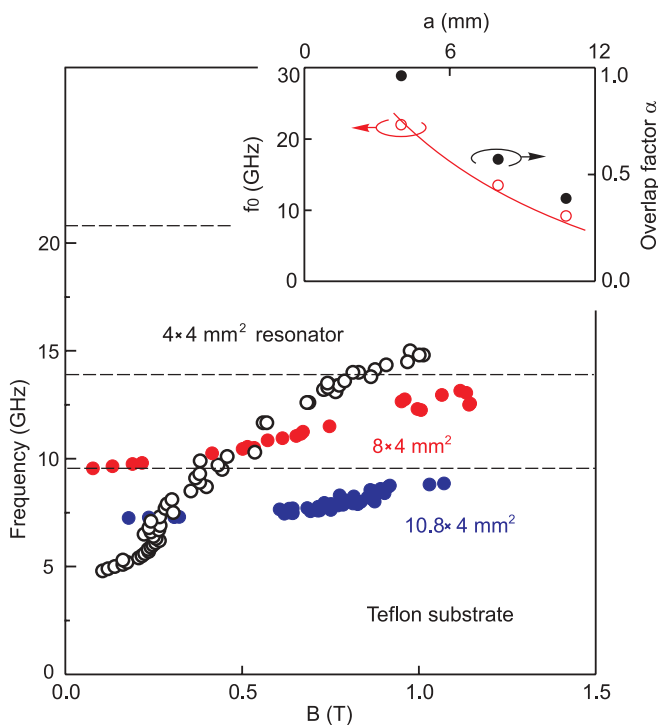


FIG. 2. (Color online) Dependences of microwave resonance frequencies on magnetic fields exhibiting transmission maxima. The different symbols correspond to different resonators on a teflon substrate: 4×4 mm², 8×4 mm², and 10.8×4 mm². The inset displays the unperturbed photon frequency and overlap factor values versus resonator size a along the 2DES stripe. The data were recorded for $L = 1.4$ mm, $W = 50$ μ m, and $n_s = 4.7 \times 10^{11}$ cm⁻².

both ω_0 and α (Fig. 2). The inset of Fig. 2 displays the obtained ω_0 and α values versus resonator size a . For 8×4 mm² and 10.8×4 mm² resonators, ω_0 was obtained directly by measuring the resonator transmission on sweeping microwave excitation frequency at $B = 6$ T. For 4×4 mm² resonator the photon frequency was obtained from the theoretical simulation. The phenomenological overlap factor α was calculated using the theoretical model Eq. (1). The line in the inset shows the photon frequency dependence predicted by the theoretical simulations. The overlap factor decreases with the increase in a , indicating that the coupling between the cavity photon mode and the polarization medium becomes weaker. Additional experiments have demonstrated that the lateral resonator size b has no effect on the polariton magnetodispersion. Therefore, α cannot be estimated simply as the ratio of the 2DES stripe and resonator areas. It is remarkable that for a 4×4 mm² resonator, the calculated overlap factor is $\alpha = 0.96$, suggesting that the 2DES stripe introduces a dominant perturbation into the field distribution of the bare resonator photon mode. Hence, the theoretical model is incapable of describing our experimental results quantitatively. However, the qualitative agreement between model and experiment is evident. We expect that a comprehensive theoretical description can be obtained if the geometry of the interaction between the photon resonator mode and 2D plasma is accounted for.

Figure 3(a) illustrates the role the patch resonator plays in the formation of cyclotron polariton modes. The filled symbols display the polariton magnetodispersion recorded when no metallic resonator is present under the semiconductor chip. The open symbols correspond to the case where this chip is placed onto a 4×4 mm² metallic resonator. In both experiments, the substrate material was ceramic and the 2DES stripe has the following parameters $L = 1.4$ mm, $W = 50$ μ m, and $n_s = 4.7 \times 10^{11}$ cm⁻². Both magnetodispersion curves have the same behavior; i.e., the mode frequency increases with the magnetic field. We conclude that the polariton mode observed in the absence of the patch resonator originates from the coupling of cyclotron plasmon with accessory high-frequency photon mode. We attribute this photon mode to an electromagnetic field resonance in the 2DES semiconductor crystal. Notably, in all of our experiments, the complementary polariton modes with a negative magnetodispersion were observed. These modes revealed themselves as very weak transmission resonances. An example of the magnetodispersion of the complementary polariton modes measured for the reference configuration (2DES stripe placed onto 4×4 mm² metallic resonator) is plotted in Fig. 3(a) by small dots. The arrow in Fig. 3(a) shows the calculated zero field frequency value of the fundamental 1D plasmon mode for the stripe under study. We interpret the observed modes as edge-magnetoplasma polariton excitations. Edge magnetoplasmons (EMPs) are plasma waves propagating along the edge of the 2DES in the direction dictated by the external B field.¹⁸⁻²⁰ Their velocity is proportional to the Hall conductivity $\sigma_{xy} \propto n_s/B$. Hence, EMPs' hallmark is their negative magnetodispersion; i.e., frequency of the mode decreases with increase in magnetic field. Observed modes have negative magnetodispersion [Fig. 3(a)], and therefore, they have edge-magnetoplasma nature. A detailed study of these modes will be a topic for our future research.

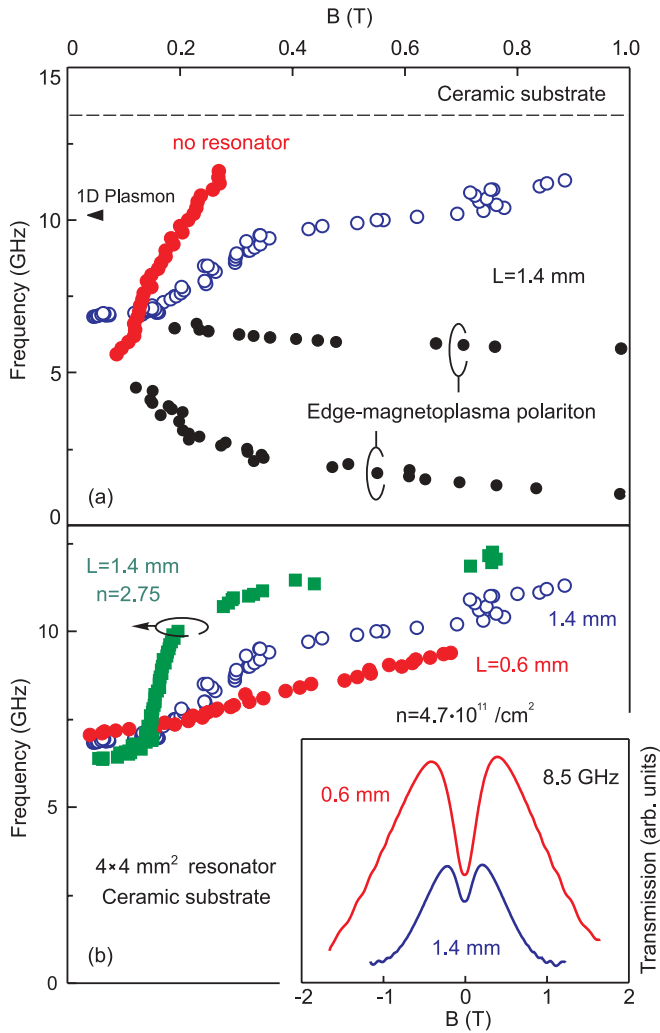


FIG. 3. (Color online) (a) Magnetodispersion of the polariton mode for a 2DES stripe placed on a $4 \times 4 \text{ mm}^2$ metallic resonator on a ceramic substrate (open symbols) and on a bare ceramic substrate (filled symbols). The small circles correspond to edge-magnetoplasma polariton modes. (b) Polariton magnetodispersion for different parameters of the 2D electron system, with a fixed resonator ($4 \times 4 \text{ mm}^2$ on a ceramic substrate). The inset shows the magnetic-field transmission dependencies of the 2DES stripes with lengths $L = 1.4 \text{ mm}$ and 0.6 mm at $f = 8.5 \text{ GHz}$.

Figure 3(b) shows the polariton magnetodispersion for the different parameters of the 2D electron system, while the resonator remains the same ($4 \times 4 \text{ mm}^2$ on a ceramic substrate). The open circle points were obtained at $L = 1.4 \text{ mm}$ and $n_s = 4.7 \times 10^{11} \text{ cm}^{-2}$ (structure 1). The filled circle points were obtained at $L = 0.6 \text{ mm}$ and $n_s = 4.7 \times 10^{11} \text{ cm}^{-2}$ (structure 2). Rectangular points were obtained at $L = 1.4 \text{ mm}$ and $n_s = 2.75 \times 10^{11} \text{ cm}^{-2}$ (structure 3). In the strong magnetic-field limit, each of these magnetodispersion curves merges into the same photonic line $\omega_0/2\pi = 13 \text{ GHz}$.

Thus, we conclude that the frequency of the polariton mode is not affected by the 2DES parameters at large magnetic fields. In the opposite small magnetic field limit, the curves extrapolate to the following zero field polariton frequencies: $f_{LP(1)} = 6.8 \text{ GHz}$, $f_{LP(2)} = 7.0 \text{ GHz}$, and $f_{LP(3)} = 6.0 \text{ GHz}$. In the limit of $\omega_p \gg \omega_0$, the theoretical considerations yield a value for the zero field polariton frequency of $\omega = \omega_0 \sqrt{1 - \alpha}$. When the length of the 2DES stripe is decreased, the corresponding α also decreases. This fact explains the rise of the polariton frequency from $f_{LP(1)}$ to $f_{LP(2)}$. Due to the decrease of the zero field polariton frequency from $f_{LP(1)}$ to $f_{LP(3)}$, we conclude that in our experiments, the $\omega_p \gg \omega_0$ limit is not fully fulfilled. Therefore, the plasmon frequency $\omega_p \sim \sqrt{n_s/W}$ influences the polariton frequency f_{LP} , although to a minor extent. In moderate magnetic fields, there is a strong difference in behavior for all three magnetodispersion curves [Fig. 3(b)]. For instance, the inset of Fig. 3(b) shows the magnetic-field transmission dependencies measured for 2DES stripes of lengths $L = 1.4 \text{ mm}$ and 0.6 mm at $f = 8.5 \text{ GHz}$. This observation is contrary to the theoretical model (Eq. 1). The model predicts that the stripe length must not have such a strong effect on the polariton magnetodispersion. A more correct physical picture of the 2DES plasma behavior in the presence of a magnetic field should be considered.⁷ The interpretation of this discrepancy is an interesting task and will be a topic for our future research.

IV. CONCLUSIONS

In conclusion, we have investigated the microwave transmission of a 2DES stripe placed on a metallic patch resonator. A low-frequency 2DES polariton excitation is detected in the ultrastrong coupling regime, $\omega_p \gg \omega_0$, distinct from previous studies.^{2,6,8,9,15} Physically, this limit corresponds to the creation of a complex excitation: a photon dressed by the electron cloud. We have shown that in zero magnetic field, the polariton frequency is determined mainly by the resonator photon frequency and the phenomenological 2DES-resonator overlap factor. It is demonstrated that existing theoretical models cannot quantitatively describe the observed polariton state. Therefore, a theory that captures the cyclotron plasmon-photon coupling geometry is highly desirable. In addition, a demonstration of an edge-magnetoplasma polariton mode is given. Obtained data are of value for researchers interested in microwave response of 2DES in low magnetic fields, for example, in the study of microwave-induced magnetoresistance oscillations.²¹ The tunability of this system under study makes it attractive for different applications operating in the ultrastrong coupling regime.

ACKNOWLEDGMENTS

This work was supported by the Russian Foundation for Basic Research, the Russian Academy of Sciences, and the President Grant for Young Scientists.

¹C. Weisbuch, M. Nishioka, A. Ishikawa, and Y. Arakawa, *Phys. Rev. Lett.* **69**, 3314 (1992).

²D. Dini, R. Kohler, A. Tredicucci, G. Biasiol, and L. Sorba, *Phys. Rev. Lett.* **90**, 116401 (2003).

- ³A. Wallraff, D. I. Schuster, A. Blais, L. Frunzio, R. S. Huang, J. Majer, S. Kumar, S. M. Girvin, and R. Schoelkopf, *Nature (London)* **431**, 162 (2004).
- ⁴J. Raimond, M. Brune, and S. Haroche, *Rev. Mod. Phys.* **73**, 565 (2001).
- ⁵C. Ciuti, G. Bastard, and I. Carusotto, *Phys. Rev. B* **72**, 115303 (2005).
- ⁶G. Günter, A. A. Anappara, J. Hees, A. Sell, G. Biasiol, L. Sorba, S. De Liberato, C. Ciuti, A. Tredicucci, A. Leitenstorfer, and R. Huber, *Nature (London)* **458**, 178 (2009).
- ⁷D. Hagenmüller, S. De Liberato, and C. Ciuti, *Phys. Rev. B* **81**, 235303 (2010).
- ⁸V. M. Muravev, I. V. Andreev, I. V. Kukushkin, S. Schmult, and W. Dietsche, *Phys. Rev. B* **83**, 075309 (2011).
- ⁹G. Scalari, C. Maissen, D. Turcinkova, D. Hagenmüller, S. De Liberato, C. Ciuti, C. Reichl, D. Schuh, W. Wegscheider, M. Beck, and J. Faist, *Science* **335**, 1323 (2012).
- ¹⁰I. V. Kukushkin, J. H. Smet, S. A. Mikhailov, D. V. Kulakovskii, K. von Klitzing, and W. Wegscheider, *Phys. Rev. Lett.* **90**, 156801 (2003).
- ¹¹I. V. Kukushkin, V. M. Muravev, J. H. Smet, M. Hauser, W. Dietsche, and K. von Klitzing, *Phys. Rev. B* **73**, 113310 (2006).
- ¹²S. A. Mikhailov and N. A. Savostianova, *Phys. Rev. B* **71**, 035320 (2005).
- ¹³L. Sapienza, A. Vasanelli, R. Colombelli, C. Ciuti, Y. Chassagneux, C. Manquest, U. Gennser, and C. Sirtori, *Phys. Rev. Lett.* **100**, 136806 (2008).
- ¹⁴M. Geiser, G. Scalari, F. Castellano, M. Beck, and J. Faist, *Appl. Phys. Lett.* **101**, 141118 (2012).
- ¹⁵Y. Todorov, A. M. Andrews, R. Colombelli, S. De Liberato, C. Ciuti, P. Klang, G. Strasser, and C. Sirtori, *Phys. Rev. Lett.* **105**, 196402 (2010).
- ¹⁶J. J. Hopfield, *Phys. Rev.* **112**, 1555 (1958).
- ¹⁷F. Stern, *Phys. Rev. Lett.* **18**, 546 (1967).
- ¹⁸D. B. Mast, A. J. Dahm, and A. L. Fetter, *Phys. Rev. Lett.* **54**, 1706 (1985).
- ¹⁹D. C. Glatli, E. Y. Andrei, G. Deville, J. Poitrenaud, and F. I. B. Williams, *Phys. Rev. Lett.* **54**, 1710 (1985).
- ²⁰V. A. Volkov and S. A. Mikhailov, *Pisma Zh. Eksp. Teor. Fiz.* **42**, 450 (1985) [*JETP Lett.* **42**, 556 (1985)].
- ²¹M. A. Zudov, R. R. Du, J. A. Simmons, and J. L. Reno, *Phys. Rev. B* **64**, 201311 (2001).